

Research Article

Development and *In Vitro* Characterization of Hyaluronic Acid-Based Coatings for Implant-Associated Local Drug Delivery Systems

Svea Petersen, Sebastian Kaule, Michael Teske, Ingo Minrath, Klaus-Peter Schmitz, and Katrin Sternberg

Institute for Biomedical Engineering, University of Rostock, Friedrich-Barnewitz-Straße 4, 18119 Rostock, Germany

Correspondence should be addressed to Svea Petersen; svea.petersen@uni-rostock.de

Received 18 January 2013; Revised 13 March 2013; Accepted 20 March 2013

Academic Editor: Zexuan Dong

Copyright © 2013 Svea Petersen et al. This is an open access article distributed under the Creative Commons Attribution License, which permits unrestricted use, distribution, and reproduction in any medium, provided the original work is properly cited.

The development of drug-eluting coatings based on hyaluronic acid (HA) is especially promising for implant-associated local drug delivery (LDD) systems, whose implantation provokes high insertion forces, as, for instance, cochlear implants or drug-coated balloons (DCB). The lubricious character of HA can then reduce the coefficient of friction and serve as drug reservoir simultaneously. In this context, we investigated several plasma- and wet-chemical methods for the deposition of HA-based coatings with LDD function on polyamide 12 as a model implant surface, conventionally used for DCB. In contrast to aminosilane, epoxy silane surface layers allowed the covalent attachment of a smooth and uniform HA base layer, which provided good adherence of further HA layers deposited by manual dip coating at a subsequent processing stage. The applied HA-crosslinking procedure during dip coating influences the transfer and release of paclitaxel, which could be reproducibly incorporated via infiltration. While crosslinking with N-(3-dimethylaminopropyl)-N'-ethylcarbodiimide hydrochloride provided HA coatings on DCB, which allowed for an efficient paclitaxel transfer upon expansion in a vessel model, crosslinking with glutaraldehyde resulted in a slower drug release being more appropriate for implants with longer residence time in the body. The developed HA coating is hence well suited for spontaneous and sustained LDD.

1. Introduction

Polymers have found applications in diverse biomedical fields such as tissue engineering, cardiovascular intervention, ophthalmology, dentistry, and bone repair [1]. Implant-associated polymer-based local drug delivery (LDD) systems, which enable controlled release of drugs into the body, are of special interest in many of these medical fields. Although vascular drug-eluting stents (DES) are probably the most commonly known example, LDD from microstents for application in the eye and the inner ear, and stimulation electrodes of cardiac pacemakers or cochlear implants, might open up new therapeutic options [2]. While principally used polymers for LDD systems are relatively hydrophobic as exemplified by the commonly used biocompatible and biodegradable polylactide [3–5], which allows for a sustained drug release over a long time period, swellable hydrophilic implant coatings are more likely used with the purpose to reduce insertion forces.

These coatings are for instance applied to angioplasty catheters for reduction of the coefficient of friction during transfer to the stenotic vessel [6]. As the spontaneous drug transfer from the so-called drug-coated balloons (DCB) is already applied as a therapeutic alternative to DES [7, 8], the development of hydrophilic coating with LDD function would be of high interest for this application. The demand can be underlined by the fact that commercially available DCB surface designs often involve water soluble additives [9, 10], which might lead to considerable drug losses during the transit of the device through the vascular system [11, 12].

Biocompatibility is a general requirement especially for implants with long residence time in the body, since the coating remains in long-term contact with the biological system, but also for DCB, as coating matrix is likely transferred with the drug to the vessel wall during expansion. With the purpose to physically maintain the drug on the implants surface during transit to the implantation site, good

adhesion of the hydrophilic coating to the implant body is a second general necessity. In contrast, requirement for drug delivery is application dependent. While an implant with longer residence time in the body should generally provide a drug release over a certain time period, DCB function via a spontaneous, and efficient drug transfer to the vessel wall during balloon expansion. The general requirement of biocompatibility might be fulfilled by using a lubricious coating based on a natural component as hyaluronic acid (HA). HA is a biodegradable, biocompatible, nontoxic, non-immunogenic and noninflammatory linear polysaccharide present in the extracellular matrix of all higher animals. In covalently crosslinked condition, HA forms a hydrophilic polymer network which may absorb a multiple of times its dry weight in water. This lubricious property combined with its biocompatibility has led to different medical applications of HA as exemplarily in ophthalmic surgery to protect delicate eye tissues during surgical manipulation [13], in orthopedics to replace synovial fluid in painful arthritis [14], and in otolaryngology to reduce insertion forces during soft-surgery cochlear implantation [15]. Moreover, formulations of HA and its derivatives are discussed in recent literature as transdermal [16] and injectable [17] vehicles for the controlled and localized drug delivery. Considering these facts, we consider HA as a promising candidate for the simultaneous provision of implants with a lubricious surface and an LDD function.

Within this context, we investigate the deposition of drug-releasing HA coatings to polyamide 12 (PA12) balloon catheter surfaces as exemplary implant application. PA12 is a popular material for balloon catheter due to its good deformability and high burst strength [18]. With the purpose to generate well-adhering HA coatings, plasma- and wet-chemical reactions are investigated with regard to the creation of functional groups on the PA12 surface, subsequent covalent attachment of a HA base layer, and resulting coating morphology. After studying the deposition of further HA layers via manual dip coating and the incorporation of paclitaxel, which has proven rapid uptake by the intima, high retention rate, and sustained biological effect when applied on DCB [19], we investigate the influence of crosslinking on spontaneous drug transfer, as afforded on DCB. In order to address the applicability of the developed HA-based LDD for implants with longer residence time in the body, drug release is also studied as a function of time.

2. Experimentals

2.1. Materials. All chemicals were purchased from Sigma-Aldrich (Taufkirchen, Germany), Mallinckrodt Baker (Griesheim, Germany), SERVA Feinbiochemica (Heidelberg, Germany), Thermo Scientific (Karlsruhe, Germany), or Merck (Darmstadt, Germany) in P.A. quality or higher if not indicated differently. HA (hyaluronic acid sodium salt from *streptococcus equi*, $M_w = 1,500,000$ Da, <1% protein impurities, Fluka, Taufkirchen, Germany) and paclitaxel (>99.5%, Cfm Oskar Tropitzsch e.K., Marktredwitz, Germany) were used as coating and model drug, respectively. The high molecular weight HA has been chosen with the aim of establishing more stable LDD systems with regard to swelling and

degradation [20]. PA12 tubes of 20 mm in length and 4 mm in diameter were drawn on glass bars of the same diameter (4 mm) for better handling and served as model implant surface during morphology, coating thickness evaluation, and drug release studies. For better visualization of the coating, a silicone tube was pulled over the PA12 tubes in order to generate a coating boundary. For contact angle measurements, infrared spectroscopy and water uptake estimation planar PA12 samples were prepared. PA12 tubes and uncoated balloon catheter of 4 mm in diameter and 20 mm in length were kindly provided by Biotronik SE & Co. KG (Erlangen, Germany).

2.2. Generation of Paclitaxel-Loaded HA Coatings on Planar and Tubular PA12

2.2.1. Silanization. With the purpose to enhance the adhesion of HA coatings to the implant surfaces, silanization with either 3-aminopropyltriethoxysilane (APTES) or 3-glycidoxypropyltrimethoxysilane (GPTMS) was performed. Therefore, PA12 samples were treated by O_2 -plasma in order to generate free hydroxyl groups at the surface (Figure 1(a)). 45 W and 3 min treatments were applied with a radio frequency plasma generator (frequency 13.56 MHz, Diener electronic GmbH & Co. KG, Ebhausen, Germany) at a low pressure of 0.3 mbar. For subsequent silanization, 4 mL of 1% (w/w) APTES (Figure 1(b)) or GPTMS (Figure 1(c)) dissolved in distilled water (dH_2O), or dry toluene, respectively, was poured over each sample and stirred for 16 h at $23 \pm 2^\circ C$. Finally, the samples were rinsed with water and dried in a vacuum chamber at $40^\circ C$ and 50 mbar overnight.

2.2.2. Chemical Attachment of a HA Base Layer to APTES-Modified Surfaces. A HA base layer was coupled to APTES-modified surfaces via the crosslinker N-(3-dimethylamino-propyl)-N'-ethylcarbodiimide hydrochloride (EDC) and N-hydroxysuccinimide (NHS) (Figure 1(d)). Therefore, samples were immersed into 4 mL of phosphate-buffered saline (Dulbecco's PBS, pH 7.2 (DPBS)) containing 5 mg HA, 6 mg EDC, and 6 mg NHS. After 1 h reaction at $23 \pm 2^\circ C$, samples were washed three times with DPBS containing 0.05% (w/w) polyoxyethylene (20) sorbitan monolaurate (DPBS/Tween 20) and dH_2O and dried in a vacuum chamber at $40^\circ C$ and 50 mbar overnight.

2.2.3. Chemical Attachment of a HA Base Layer to GPTMS-Modified Surfaces. Chemical attachment of a HA base layer to GPTMS-modified surfaces afforded no crosslinker and was achieved via direct reaction of terminal epoxy groups at the modified surface and hydroxyl groups of HA (Figure 1(e)). Therefore, samples were immersed into 4 mL dH_2O containing 5 mg HA after adjustment of the pH the by addition of 0.1 M HCl to pH 6. After 1 h reaction at $65^\circ C$, samples were washed three times with DPBS/Tween 20 and dH_2O and dried in a vacuum chamber at $40^\circ C$ and 50 mbar overnight.

2.2.4. Dip Coating of Further HA Layers and Crosslinking. After chemical attachment of the HA base layer, further HA layers were deposited to the modified surfaces via manual

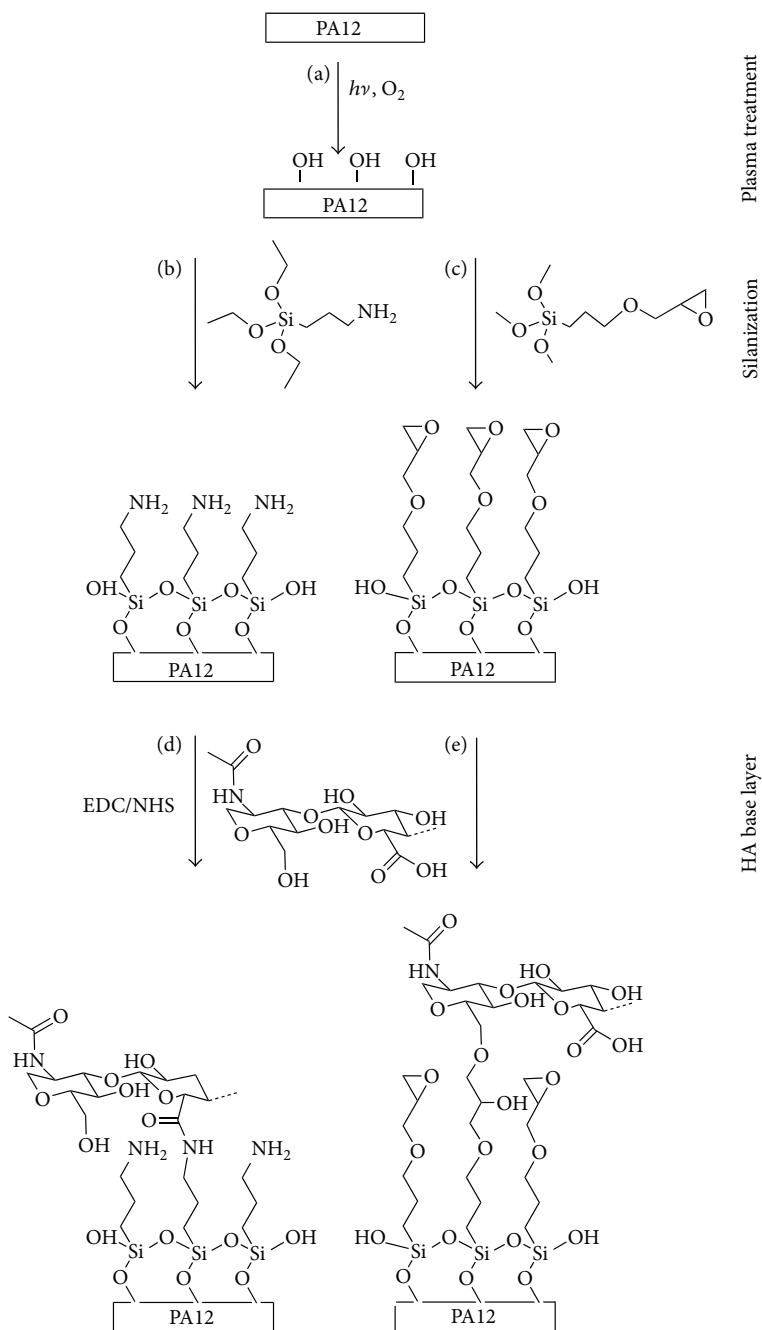


FIGURE 1: Reaction scheme for chemical attachment of a HA base layer to PA12 surfaces via (a) O_2 -plasma treatment, silanization with (b) APTES or (c) GPTMS, and covalent binding of HA via (d) activation of the carboxylic acid of HA with EDC/NHS and subsequent reaction with terminal amine groups on the APTES-modified PA12 surface or via (e) direct reaction of terminal epoxy groups at the GPTMS-modified PA12 surface and hydroxyl groups of HA.

dip coating. After each dipping process into 5 mg/mL HA in DPBS for 30 s, samples were either immersed for 5 min into a 1 Mm EDC/NHS solution in DPBS or an aqueous 25% (v/v) glutaraldehyde (GDA) solution adjusted to pH 4 by the addition of 0.1 M HCl for crosslinking (Figures 2(a) and 2(b)). The dipping process was repeated ten times with drying for 5 min at $23 \pm 2^\circ C$ after each dipping process. Finally, samples were washed again three times with DPBS/Tween 20 and

dH_2O and dried in a vacuum chamber at $40^\circ C$ and 50 mbar overnight.

2.2.5. Drug Incorporation. Incorporation of paclitaxel within the HA coatings was performed by immersion into $900 \mu L$ of ethanol/ dH_2O (8/2 (v/v)) mixture, containing 15 mg/mL paclitaxel for 16 h. This solvent mixture has been chosen as it provides good paclitaxel stability and enough swelling of

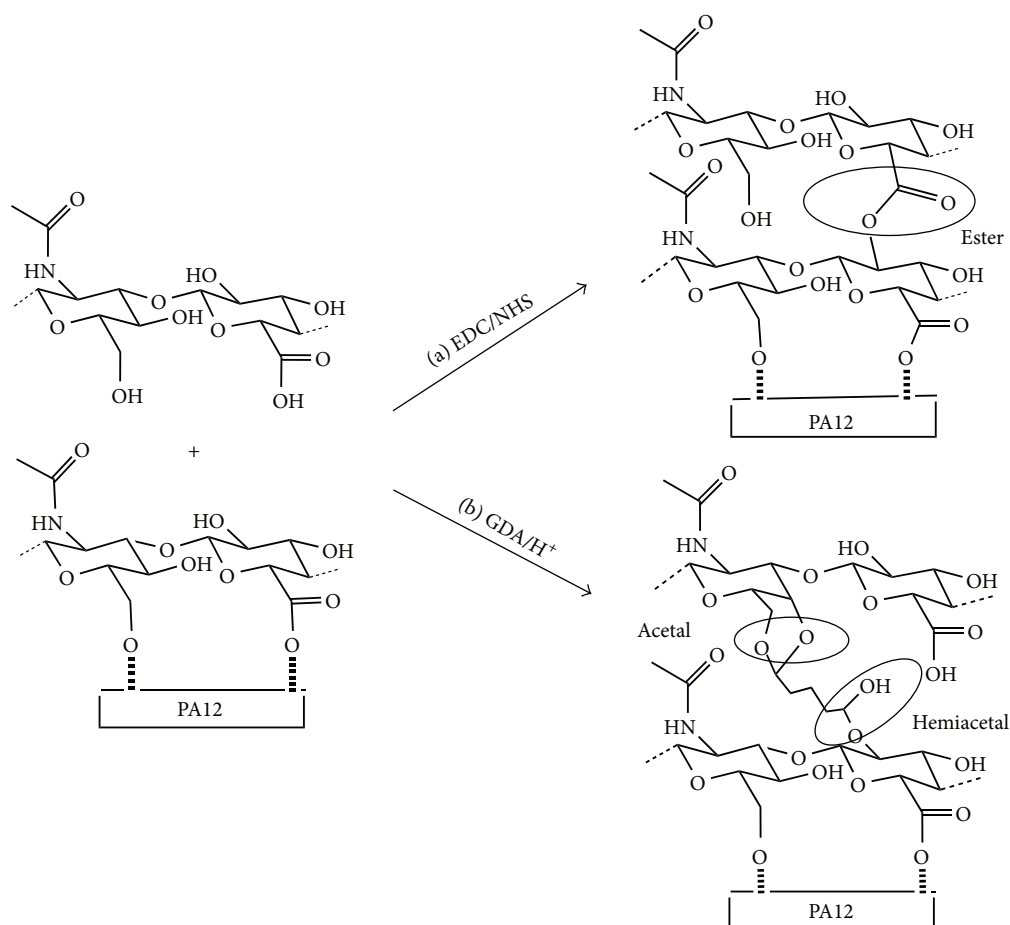


FIGURE 2: Reaction scheme for crosslinking the surface-bound HA base layer with further HA layers via (a) EDC/NHS under the formation of ester bonds or (b) GDA under the formation of hemiacetal or acetal linkages.

the hydrogel allowing interpenetration of the drug (data not shown).

2.3. Generation of Paclitaxel-Loaded HA Coatings on DCB.

The modification of balloon catheter followed the same coating procedure as described previously. After plasma-chemical treatment and prior to silanization, balloons were dilated via a manual pump ($p = 2$ bar). The air was released after the whole coating procedure.

2.4. Characterization

2.4.1. Scanning Electron Microscopy. Examination of the coating morphology was carried out in a Philips XL 30 ESEM (Philips Electron Optics, Eindhoven, The Netherlands), operating in the ESEM mode at four different positions along the coating. Representative micrographs are shown.

2.4.2. Confocal Microscopy. The evaluation of the coating thickness was performed with PA12 tubes, which have been sputtered with gold (Agar Sputter Coater, Agar Scientific, Essex, UK 0,2 bar, 15 mA, 120 s, argon atmosphere) prior to the whole coating procedure described previously. This allows for better differentiation between the PA12 surface

and the hydrogel. As morphological comparison to hydrogel coatings applied to bare PA12 does not reveal any differences, this modification was assumed to be appropriate. The coating thickness was measured on two positions along the PA12 surface by means of the microscope LEXT OLS 3000 (Olympus, Hamburg, Germany). At both positions, the coating thickness was determined by ten different measurements by means of the objective Plan Achromat MP lan Apo 100 \times numerical aperture 0.95. 1.5 has been assumed to be refractive index of the hydrogel coating.

2.4.3. Contact Angle Measurements. For the contact angle measurements, optical tensiometry (goniometry) was used, which involves the observation of a sessile drop of a test liquid on the solid substrate. Ultrapure water was chosen as test liquid. The sessile drop measurements were performed at $23 \pm 2^\circ\text{C}$. Drop volume was about $10 \mu\text{L}$. Contact angle measurements were made using the Contact Angle System OCA 20, (DataPhysics Instruments GmbH, Flinders, Germany) with five samples for each modification.

2.4.4. Fourier Transformation Infrared Spectroscopy. Surface modifications were analyzed by FTIR-ATR spectroscopy using an Equinox 55 FTIR spectrometer (Bruker Optics,

Ettlingen, Germany) equipped with a germanium crystal ATR unit and a dry air purged chamber. IR spectra were recorded in a range from $4,000\text{ cm}^{-1}$ to $1,000\text{ cm}^{-1}$ at 2 cm^{-1} resolution the by use of the OPUS 6.0 software. For each spectrum, 100 scans were averaged.

2.4.5. Oven-Based Karl Fischer (KF) Titration. Before the KF measurements were conducted, each sample was weighed using a microbalance (UMX5, Mettler Toledo, Giessen, Germany) in order to enable the indication of water uptake per mg HA coating. Then, coatings were contacted for 1 min, 2 min and 1 h with 1 mL DPBS/Tween 20 and thereafter carefully dried to remove water droplets from the surface. Samples were subsequently placed in the sample holder of the drying oven D0308 (Mettler Toledo, Gießen, Germany) and heated up to 230°C in an argon atmosphere. The water content was finally determined using a Karl-Fischer Coulometer C20 (Mettler Toledo, Gießen, Germany) with the Hydranal-Coulomat AG KF reagent (Sigma-Aldrich, St. Louis, USA). All measurements were performed in three replicates. The water uptake was calculated as the difference in the water content of samples contacted with the aqueous solutions and the noncontacted as prepared samples.

2.5. In Vitro Drug Release Study

2.5.1. Drug Loss, Transfer, and Load of HA-Based DCB. To estimate the performance of HA-based DCB, losses of paclitaxel by simple elution, as occurring during DCB insertion, were determined. Therefore, balloons of both crosslinking methods ($n = 4$) were firstly dipped in 20 mL of DPBS/0.06% (w/w) Tween 20 for 1 min at $23 \pm 2^\circ\text{C}$. In a second step, the balloons were dilated for 30 s to 7 bar in a silicone tube (outer diameter: 4.1 mm, inner diameter: 2.7 mm) in 20 mL DPBS/0.06% (w/w) Tween 20. Prior to HPLC measurement, samples were diluted 1 : 1 with methanol. Drug residue on the silicone tube and on the balloon was examined afterwards by paclitaxel extraction in 3 mL and 20 mL methanol, respectively, for 1 h at 37°C . Stated values for the transfer of paclitaxel in the silicone tube present the sum of the paclitaxel amount found in DPBS/0.06% (w/w) Tween 20 during dilatation and in the methanol extract of the silicone tube. Total drug load represents the sum of all measured paclitaxel amounts.

2.5.2. Release Kinetics. The time course of release of paclitaxel was determined from PA12 test tubes for both crosslinking methods ($n = 3$) at $23 \pm 2^\circ\text{C}$ in DPBS supplemented with 0.06% (w/w) Tween 20, which assured paclitaxel stability over a time period of in minimum 4 days as determined in preliminary experiments (data not shown). Individual samples were immersed in 20 mL elution medium for a total duration of at least 8 h. The elution medium was renewed at periodic intervals in order to ensure the maintenance of sink conditions. The drug amount released at each time period was determined by high performance liquid chromatography (HPLC), applying conditions described below, after 1 : 1 dilution with methanol. Remaining drug content after the drug release studies was evaluated by two successive extractions

TABLE 1: Contact angles of the modified planar PA12 surfaces ($n = 5$) in preparation for and after chemical attachment of the HA base layer and after deposition of crosslinked HA coatings. Data shown as mean \pm SD.

| | Unmodified | APTES | GPTMS |
|--------------------------------|------------|------------|-------------|
| Without HA | 84 ± 9 | 78 ± 9 | 78 ± 9 |
| HA base layer | 73 ± 7 | 70 ± 8 | 50 ± 10 |
| EDC/NHS-crosslinked HA coating | n.d. | n.d. | 43 ± 7 |
| GDA-crosslinked HA coating | n.d. | n.d. | 49 ± 9 |

in 10 mL and in 4 mL methanol for 30 min and 60 min at $23 \pm 2^\circ\text{C}$, respectively.

2.5.3. HPLC Parameters. $20\ \mu\text{L}$ of the test solutions was injected into an Eurospher column 100-5, C18, $120 \times 4\text{ mm}$ ID (Wissenschaftlicher Gerätebau Dr.-Ing. Herbert Knauer GmbH, Berlin, Germany). The chromatographic conditions were column temperature 23°C , isocratic eluent PBS (0.005 M, pH 3.5)/acetonitrile 50/50% (v/v), flow rate 1.0 mL/min, and UV detection at 230 nm with calibrated measurement range 0.5–20.0 mg/L and detection limit approximately 0.05 mg/L.

3. Results

3.1. Chemical Changes on Planar PA12 Surfaces in Preparation for and after Attachment of the HA Base Layer and after Deposition of Crosslinked HA Coatings. Contact angle measurements were performed in order to evaluate surface changes and the resulting hydrophilic/hydrophobic character after silanization via APTES and GPTMS and attachment of the HA base layer. For untreated PA12, a contact angle of $84 \pm 9^\circ$ was determined (Table 1). After both silanization procedures, APTES and GPTMS, no considerable change in contact angle was observed (APTES and GPTMS: $78 \pm 9^\circ$, Table 1). Surfaces became however more hydrophilic after the attachment of the HA base layer. The contact angles decreased to $73 \pm 7^\circ$ for unmodified, $70 \pm 8^\circ$ for APTES-modified and $50 \pm 10^\circ$ for GPTMS-modified PA12 surfaces (Table 1).

The recorded IR spectrum of the untreated PA12 showed clear signals at $2,900\text{ cm}^{-1}$ and $2,850\text{ cm}^{-1}$ which were affiliated with the presence of $-\text{CH}_2$ groups within the polyamide network (Figure 3) and at $1,650\text{ cm}^{-1}$ resulting from the stretch vibration of the $-\text{C}=\text{O}$ (Figure 2). PA12 to which a HA base layer was chemically attached via GPTMS presented an additional small peak at $1,040\text{ cm}^{-1}$ and a broad vibration band at $3,300\text{ cm}^{-1}$ assigned to ether ($-\text{C}-\text{O}-\text{C}-$) and hydroxyl ($-\text{O}-\text{H}$) stretching within HA (Figure 3). Interestingly, neither APTES-modified nor unmodified PA12 surfaces revealed these bands after HA attachment (data not shown). The spectrum of the pure PA12 revealed in contrast a narrower band at $3,300\text{ cm}^{-1}$ originating from the N-H stretch vibration.

APTES-modified surfaces were not examined for the deposition of further HA layers due to the bad appearance of the HA base layer. The deposition of the HA coating to

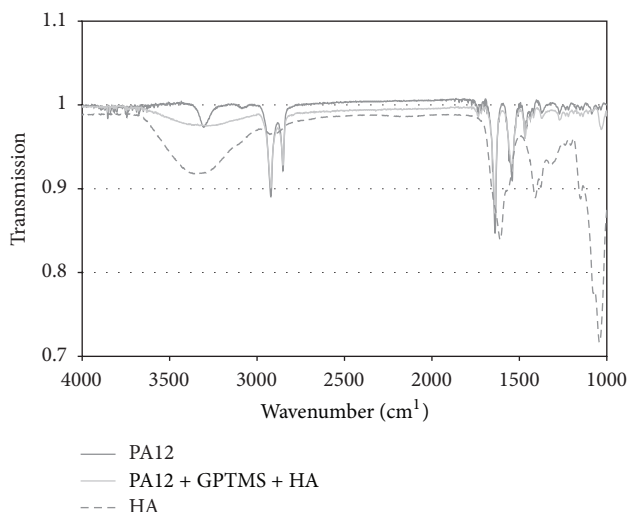


FIGURE 3: FTIR-ATR spectra of PA12 prior to and after chemical attachment of the HA base layer via GPTMS in comparison to HA.

GPTMS-modified surfaces did not change considerably the resulting contact angle (Table 1) and IR spectra.

3.2. Surface Morphology of the HA Base Layer on PA12 Tubes. The surface morphology of the HA base layer on APTES- and GPTMS-modified surfaces was assessed on PA12 tubes in comparison to unmodified surfaces at the coating boundary for better visualization. Representative ESEM micrographs revealed a well-visible coating boundary on GPTMS-modified surfaces (Figure 4(c)). The coating itself seemed smooth and homogeneous. In contrast, the coating boundary was less visible on APTES-modified surfaces and hardly visible on unmodified surfaces (Figures 4(a) and 4(b)). The coating appeared very thin on these two surfaces. In all cases, coating thickness could be hardly determined by confocal microscopy, indicating that all HA base layers including the one on GPTMS-modified surfaces were probably below $1\ \mu\text{m}$. A representative height profile of the HA base layer in GPTMS-modified surfaces is demonstrated in Figure 6(a).

3.3. Surface Morphology of the Crosslinked HA Coating on PA12 Tubes and DCB. The manual dip coating of further HA layers to the chemically attached HA base layer on GPTMS-modified surfaces was monitored via electron microscopy. After each HA layer, crosslinking with either EDC/NHS or GDA was performed. Representative ESEM micrographs of an EDC/NHS-crosslinked HA coating demonstrated a very smooth, homogeneous, and uniform coating, which was hardly visualizable without an intentionally created scratch (Figures 5(a), 5(b), and 5(d)). For comparison, the HA coating deposited on unmodified PA12 was chipping off the surface at multiple sites (Figure 5(b)). GDA-crosslinked HA coatings had a similar appearance as the demonstrated EDC/NHS-crosslinked coating (data not shown). Furthermore, the deposition of both coatings, EDC/NHS and GDA crosslinked, led to an increase in coating thickness. Height profiles determined by confocal microscopy reveal mean

TABLE 2: Water uptake of EDC/NHS- and GDA-crosslinked HA coatings ($n = 3$) after different swelling times in 1 mL PBS/Tween 20. Data shown in mg water per mg coating as mean \pm SD.

| Swelling time | EDC/NHS-crosslinked HA coating | GDA-crosslinked HA coating |
|---------------|--------------------------------|----------------------------|
| 1 min | 5.04 ± 0.17 | 1.90 ± 0.25 |
| 2 min | 5.27 ± 0.70 | 2.61 ± 0.15 |
| 1 h | 6.78 ± 0.39 | 3.21 ± 0.33 |

coating thicknesses of $2.79 \pm 0.18\ \mu\text{m}$ and $2.70 \pm 0.14\ \mu\text{m}$ for EDC/NHS- and GDA-crosslinked HA coatings, respectively (Figures 6(b) and 6(c)). Interestingly, no thickness increase could be observed for samples omitting the crosslinking procedure during dip-coating, the height profile has the same appearance as the one of the base layer (Figure 6(a)). The coating strategy has been also applied to PA12 balloon catheter. A representative photograph is shown in Figure 7(a). ESEM evidenced comparative coating morphology as observed on modified PA12 tubes (data not shown).

3.4. Water Uptake of Crosslinked HA Coatings. Water uptake of EDC/NHS- and GDA-crosslinked HA coatings was estimated via oven-based Karl Fischer titration after different swelling times in the *in vitro* release medium DPBS/Tween 20. While both coatings showed an increase in water uptake with increasing swelling time, EDC/NHS-crosslinked HA coatings took up twice as much water as GDA-crosslinked HA coatings (Table 2).

3.5. In Vitro Paclitaxel Loss and Transfer from Differently Crosslinked HA Coatings on GPTMS-Modified PA12 Balloon Catheter. To estimate the performance of HA-based DCB, losses of paclitaxel during 1 min elution in aqueous medium, as occurring during balloon catheter insertion and drug transfer upon expansion in a silicone tube as model for the stenotic vessel were determined. With $10 \pm 2\ \mu\text{g}$ paclitaxel from EDC/NHS- and $6 \pm 1\ \mu\text{g}$ paclitaxel from GDA-crosslinked HA coatings, relative drug losses during elution were lower than 5% of the initial drug load for both coatings (Figure 7(b)). Paclitaxel transfer upon expansion of the DCB in a silicone tube was in contrast considerably enhanced for EDC/NHS-crosslinked HA coatings. In total, $141 \pm 45\ \mu\text{g}$ paclitaxel (50% of the initial drug load) were transferred to the silicone tube from EDC/NHS-crosslinked HA coatings, while GDA-crosslinked HA coatings evidenced a transfer of $22 \pm 1\ \mu\text{g}$ paclitaxel (8% of the initial drug load). Total drug load was $279 \pm 27\ \mu\text{g}$ for EDC/NHS- and $283 \pm 4\ \mu\text{g}$ for GDA-crosslinked HA coatings. As investigated, DCB had a size of $4 \times 20\ \text{mm}$, a paclitaxel dose of approximately $1.1\ \mu\text{g}/\text{mm}^2$ was assumed for both coatings.

3.6. In Vitro Paclitaxel Release from Differently Crosslinked HA Coatings on GPTMS-Modified PA12 Tubes. The performed *in vitro* release studies demonstrated that differently crosslinked HA coatings discharged the incorporated paclitaxel in a different manner (Figure 7(c)). EDC/NHS-crosslinked HA

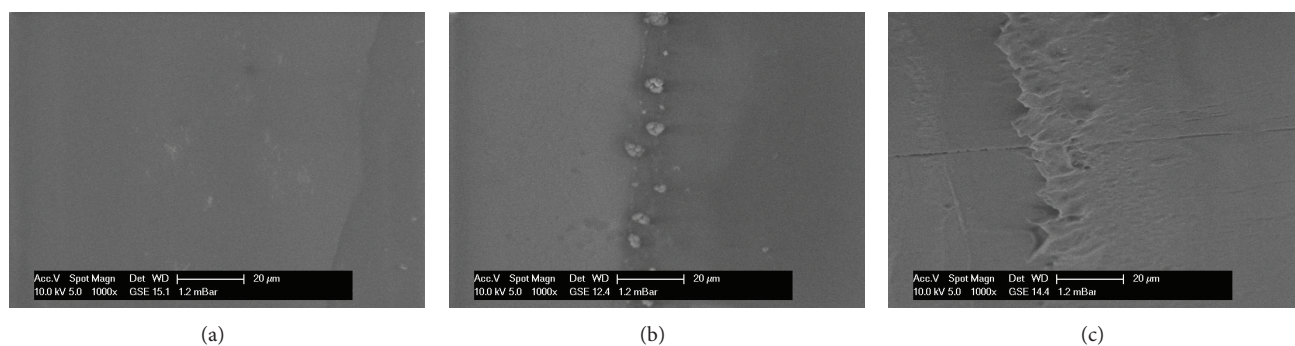


FIGURE 4: Representative ESEM micrographs of HA base layer coupled to (a) unmodified, (b) APTES-modified, and (c) GPTMS-modified PA12 surfaces. For better visualization of the coating, the coating boundary was put into focus. Attachment of HA to unmodified surfaces was performed according to conditions for GPTMS-modified surfaces.

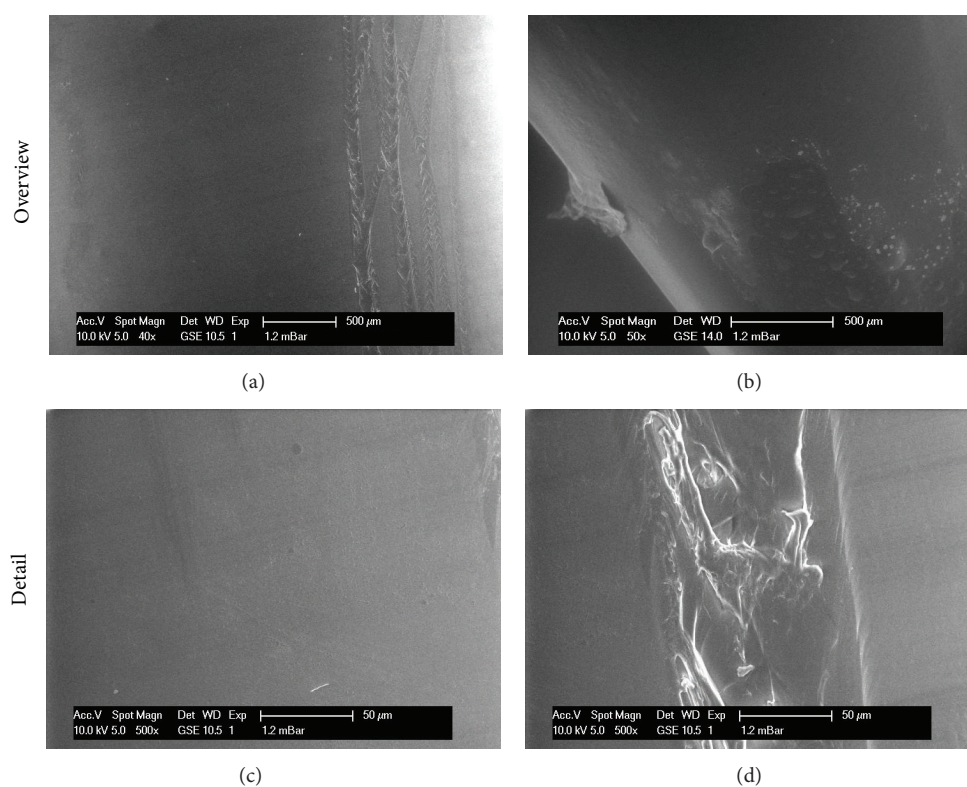


FIGURE 5: Representative ESEM micrographs of EDC/NHS-crosslinked HA coatings on (a), (c), and (d) GPTMS-modified and (b) unmodified surfaces. The scratch on GPTMS-modified surfaces (a) and (d) has been done intentionally for a better visualization of the coating.

coatings revealed a faster paclitaxel release rate than GDA-crosslinked HA coatings. While the drug depot of EDC/NHS-crosslinked HA coatings was already exhausted after 0.75 h, GDA-crosslinked HA coatings provided drug release for over 4 h. The determined total drug load was $261 \pm 25 \mu\text{g}$ for EDC/NHS- and $284 \pm 11 \mu\text{g}$ for GDA-crosslinked HA coatings.

4. Discussion

In order to provide implants including a hydrophilic lubricant coating with an LDD function, we aimed at the development of a stable good adhering HA coating with reproducible drug

incorporation and release properties to PA12 model implant surfaces. As such coatings would be interesting for spontaneous as well as for sustained LDD, we aimed at the adjustment of the release characteristics by applying two different crosslinking procedures.

For this purpose, plasma- and wet-chemical methods were established to activate the PA12 surface in order to generate functional groups which are able to covalently attach to a HA base layer. This should provide good adherence of further HA layers deposited by manual dip coating at a subsequent processing stage. First, an activation step by O_2 plasma was established in order to generate $-\text{OH}$ groups on the PA12 surface that act as reactive terminal groups for

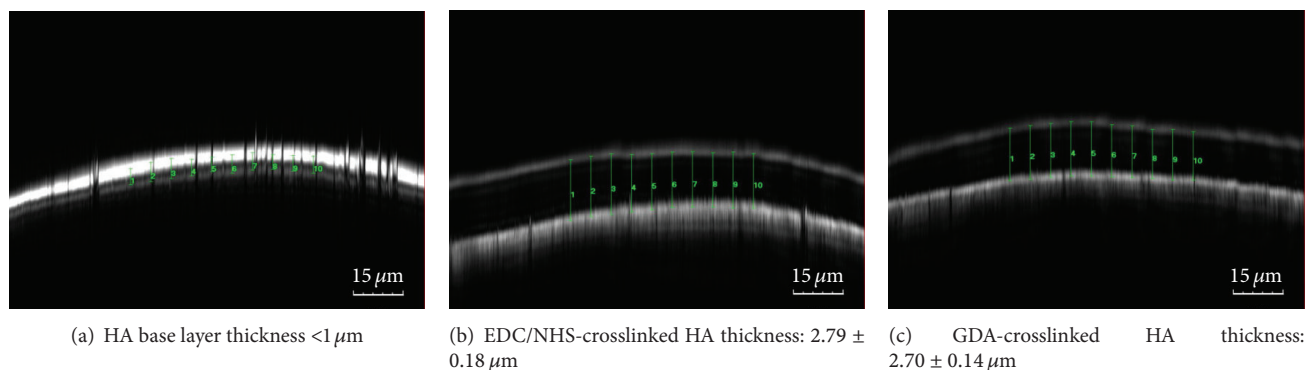


FIGURE 6: Representative height profiles (xz scans) determined by confocal microscopy of (a) HA base layer, (b) EDC/NHS-crosslinked HA coatings, and (c) GDA-crosslinked HA coatings on GPTMS-modified surfaces. The indicated thickness \pm standard deviation has been averaged over 2 positions along the PA12 tube with each ten measurement points.

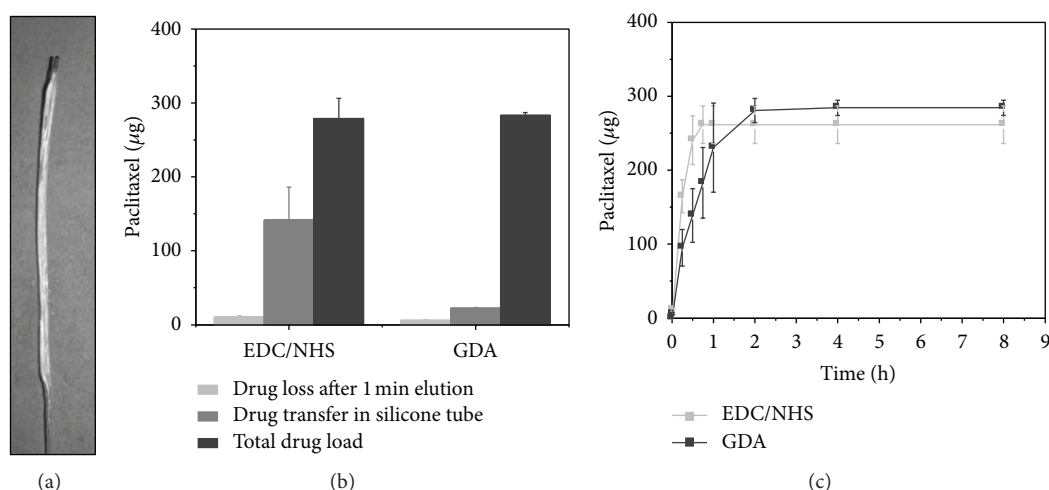


FIGURE 7: (a) Representative photograph of an EDC/NHS-crosslinked HA coating on GPTMS-modified PA12 balloon catheter, (b) paclitaxel loss after one minute elution in DPBS/Tween-20, paclitaxel transfer upon expansion in silicone tube (30 s, 7 bar) and total drug load of EDC/NHS- and GDA-crosslinked HA coatings on GPTMS-modified PA12 balloon catheter ($n = 4$) at $23 \pm 2^\circ\text{C}$, all data shown as mean \pm SD, and (c) *in vitro* paclitaxel release from EDC/NHS- and GDA-crosslinked HA coatings on GPTMS-modified PA12 tubes ($n = 3$) in DPBS/Tween 20 at $23 \pm 2^\circ\text{C}$.

the following silanization with APTES and GPTMS. After the treatment with either APTES or GPTMS, the contact angle did not change considerably with regard to unmodified PA12 (Table 1). Though both silanes present hydrophilic head groups, they have a generally more hydrophobic character comparable to PA12. After chemical attachment of the HA base layer, the contact angle decreased furthermore, indicating the successful attachment of the hydrophilic HA. As the contact angle on GPTMS-modified PA12 was smaller than on APTES-modified PA12, chemical attachment of HA seemed to be more efficient to GPTMS than to APTES. Unspecific attachment of HA to unmodified surfaces, monitored for comparison, led to a comparable contact angle as determined after attachment of HA to APTES-modified surfaces. FTIR-ATR spectra supported this tendency (Figure 3). While surfaces to which a HA base layer was chemically attached via GPTMS presented an additional small peak at $1,040 \text{ cm}^{-1}$ and a broad vibration band at $3,300 \text{ cm}^{-1}$ assigned to ether

($-\text{C}-\text{O}-\text{C}-$) and hydroxyl ($-\text{O}-\text{H}$) stretching within HA, neither APTES-modified nor unmodified PA12 surfaces revealed any changes in comparison to spectra recorded prior to HA base layer attachment. The observation of the HA peaks using FTIR-ATR spectroscopy indicated that a relatively thick layer of HA was present on GPTMS-modified surfaces, since Ångstrom-scale organic layers on polymers would be very difficult to be detected by this technique. Thus, the simplistic monolayer model portrayed in Figure 1 indicates only the sequence of attachment events, but does not represent the complexity of the attached layer. For instance, it is known that alkoxysilanes cannot only condense with the surface residues to form siloxane linkages, but also condensate with each other and build oligomers in solution prior to condensation with the solid substrate [21]. Multilayer formation is a logical consequence.

ESEM micrographs confirmed the aforementioned formation of a thicker HA layer on GPTMS than on

APTES-modified surfaces (Figure 4). Confocal microscopy did however hardly allow for an estimation of the coating thickness, which provokes the assumption that the base layer is less than $1\ \mu\text{m}$. That epoxy silane self-assembled monolayers (SAM) may serve as a molecularly smooth template for chemical tethering of composite polymer layers has been demonstrated in general [22] and applied for the covalent immobilization of HA via conversion of the surface epoxy groups to aldehydes and reaction with HA through an adipic dihydrazide linkage [23]. In the present study, we aimed at a direct reaction of terminal epoxy groups at the surface and hydroxyl or carboxyl groups of HA, as commonly used to crosslink HA by means of diepoxy compounds [24–26]. The reaction was hence straightforward and might occur at five different reaction sites per HA monomer. The attachment of HA to amino groups on APTES-modified surfaces in contrast afforded preactivation of the one carboxyl group per HA monomer with a carbodiimide [27], which might lower the reaction probability being a possible explanation of the better performance of GPTMS for HA binding. The following deposition of further crosslinked HA layers by manual dip coating was hence only examined on GPTMS-modified surfaces. Therefore, modified surfaces were ten times alternately dipped into an HA solution for 30 s and then into a solution containing either EDC/NHS or GDA as crosslinking agents for 5 min. The successful deposition of further HA layers could be evidenced by an increase of coating thickness determined by confocal microscopy. Independently, of the applied crosslinker a similar final coating thickness was determined in dried condition (Figures 6(b) and 6(c)). Thus, the amount of HA deposited was only defined by the PA12 surface wettability and the HA adhesion during the 30 s dip-coating process. As no thickness increase could be observed for samples omitting the crosslinking procedure during dip-coating, crosslinking seemed to be successful under chosen experimental conditions.

With carbodiimides, the crosslinking occurs through the initial formation of O-acylisourea on the HA carboxyl group. Either reaction with NHS yielding the formation of an NHS ester or with neighboring carboxyl groups yielding the formation of an anhydride is then thinkable as a next step. Both intermediates are able to react with hydroxyl groups when being in close contact resulting in the constitution of the ester bond [24, 28] (Figure 2(a)). With GDA, it is thought that crosslinking of HA occurs by formation of hemiacetal linkages between the aldehyde groups of GDA and hydroxyl groups of HA, which might be even transformed to the more stable acetal linkages [24] (Figure 2(b)). That crosslinking successful under chosen experimental conditions can be probably dedicated to the fact that crosslinking agents diffused into the deposited hydrogel during each of the ten crosslinking steps. Consequently, the initializing reaction as well as the final crosslinking might still proceed within the deposited hydrogel during the whole dip-coating process (approximately 2 h), which also guaranteed close contact of functional groups.

Morphological characterization of the deposited crosslinked HA layers by scanning electron microscopy revealed

smooth and homogeneous coatings on the GPTMS-modified surfaces, which were hardly visualizable without the intentionally applied scratch. The HA coating deposited on unmodified PA12 was in contrast chipping off the surface at multiple sites (Figure 5). The chemical surface modification hence allowed for better adherence of the HA coating to PA12. At the example of DCB, this is essential on one hand to allow for an efficient reduction of the coefficient of friction during transfer to the stenotic vessel and on the other hand to physically maintain the drug on the balloon surface until reaching the intended site of drug transfer.

In order to estimate the applicability of the developed HA coating for DCB, losses of paclitaxel by simple elution, as occurring during balloon catheter insertion but not preferentially in the stenotic vessel, and drug transfer upon expansion in a silicone tube as model for the stenotic vessel could be determined. While HA crosslinking seemed to have no meaningful impact on the drug loss, which was low for both tested groups, drug transfer was found to be considerably elevated for DCB with an EDC/NHS compared to DCB with a GDA-crosslinked HA coating (Figure 7(b)). 50% of the initial paclitaxel load could be transferred from EDC/NHS-crosslinked HA coatings upon expansion within 30 s corresponding to a realistic time during cardiovascular intervention. Although data might not be directly correlated to *in vivo* performance, this amount seems promising as values of *in vivo* drug transfer from commercially available DCB reported by Kelsch et al. and Scheller et al. are as low as 20% and 17% respectively of the initial drug load [7, 11].

As discussed previously for the attachment of the HA base layer the presence of five different reaction sites (hydroxyl groups) per HA monomer during crosslinking with GDA might have enhanced reaction probability versus one reaction site (carboxyl group) per HA monomer during EDC/NHS-crosslinking. A lower crosslinking generally allows for a higher swelling in aqueous medium and hence a higher spontaneous paclitaxel transfer upon balloon expansion in the silicone tube. Water uptake data determined by Karl Fischer titration after 2 min contact with the release medium, corresponding to the time of balloon preelution, insertion into the silicone tube, and 30 s expansion, corroborated this statement. EDC/NHS-crosslinked coatings, allowing more efficient transfer of paclitaxel upon balloon expansion, took up to 5.27 mg water per mg coating, while GDA-crosslinked coatings only took up to 2.61 mg/mg (Table 2). Interestingly, we however did not observe differences in drug load, probably as both coatings were saturated with paclitaxel after the 16 h applied for drug incorporation. Recorded *in vitro* drug release data in contrast corresponded to the drug transfer studies from DCB, since EDC/NHS-crosslinked HA coatings provided a faster drug release than GDA-crosslinked HA coatings with both drug depots being exhausted after less than 4 h (Figure 7(c)). Besides the above-mentioned swelling behavior, stability of chemical bonds within the hydrogel network might have also contributed to the differences observed during the *in vitro* drug release study. For instance, ester bonds formed by EDC/NHS crosslinking tend to hydrolyze under chosen drug release conditions (pH 7.2), while acetal linkages are rather stable at neutral to basic pH. If the GDA

crosslinking conditions hence allowed for the generation of acetal besides hemiacetal linkages, this fact also explains the faster drug release observed from EDC/NHS compared to GDA-crosslinked HA coatings.

In comparison to the relatively hydrophobic polymers, conventionally used for LDD, observed drug release rates were thus very high due to the crosslinking-independent hydrophilic character of HA. The HA coating can be hence used to provide high drug concentrations in the initial phase immediately after implantation. Combination with a sustained release from the implant body, as we recently proposed for the release of dexamethasone from silicone-based electrode carriers of cochlear implants, is however conceivable [29].

The observed correlation of a higher crosslinking degree with a slower drug release rate has been already described in the literature [30]. The implementation of further HA crosslinking procedures [24] can be accordingly used for further drug release adjustment with regard to each application. Generally, one can however state that a lower degree of crosslinking is recommended for the coating of implants which should provide a spontaneous drug transfer while a high degree of crosslinking is advisable for implants which should provide a sustained drug release over a certain time period.

5. Conclusion

The development of drug-eluting HA coatings is especially promising for implant-associated LDD systems, whose implantation provokes high insertion forces. The lubricious character of HA can then reduce the latter and serve as drug reservoir simultaneously. Processing time and cost could be hence possibly reduced. Within the present study, we could develop such a coating for the exemplary application of DCB, combining good adherence to the balloon surface and promising drug transfer results upon expansion. By the application of different HA-crosslinking agents and conditions, the drug transfer/release properties of the coating can be however adjusted with regard to the application. While a lower degree of crosslinking seems to be adequate for the coating of implants, which should provide a spontaneous drug transfer as DCB, a high degree of crosslinking is more advisable for implants, which should provide a sustained drug release over a certain time period. Moreover, transferability of the developed coating strategy to other implant surfaces than PA12 is likely possible, since the applied plasma- and wet-chemical modifications have been already discussed for several polymers including silicone [31]. Hence, coating of silicone-based cochlear electrode carrier for efficient reduction of insertion forces and prevention of fibrosis presents a further promising application prospect of the developed drug-eluting HA coating.

Abbreviations

APTES: 3-Aminopropyltriethoxysilane
 DCB: Drug-coated balloon
 DES: Drug-eluting stents

EDC: N-(3-Dimethylaminopropyl)-N'-ethylcarbodiimide hydrochloride
 GDA: Glutardialdehyde
 GPTMS: Glycidoxypropyltrimethoxysilane
 HA: Hyaluronic acid
 LDD: Local drug delivery
 NHS: N-Hydroxysuccinimide
 PA12: Polyamide 12.

Acknowledgments

The authors thank Thomas Reske, Martina Schröder, and Janine Schmidt for their expert technical assistance, Andreas Hofmann for his helpful suggestions, and the Biotronik SE and Co. KG, Erlangen, Germany, for the generous supply of PA12 tubes and the uncoated balloon catheter. Furthermore, financial support by Bundesministerium für Bildung und Forschung (BMBF) within REMEDIS "Höhere Lebensqualität durch neuartige Mikroimplantate" (FKZ: 03IS2081) and TheraNova (FKZ: V-630-S088-2010/268) is gratefully acknowledged.

References

- [1] J. Jagur-Grodzinski, "Biomedical application of functional polymers," *Reactive and Functional Polymers*, vol. 39, no. 2, pp. 99–138, 1999.
- [2] K. Sternberg, S. Petersen, N. Grabow et al., "Implant-associated local drug delivery systems for different medical applications," *Biomedizinische Technik*, vol. 57, Supplement 1, pp. 393–396, 2012.
- [3] C. M. Bünger, N. Grabow, C. Kröger et al., "Iliac anastomotic stenting with a sirolimus-eluting biodegradable poly-L-lactide stent: a preliminary study after 6 weeks," *Journal of Endovascular Therapy*, vol. 13, no. 5, pp. 630–639, 2006.
- [4] K. Sternberg, S. Kramer, C. Nischan et al., "In vitro study of drug-eluting stent coatings based on poly(L-lactide) incorporating cyclosporine A—drug release, polymer degradation and mechanical integrity," *Journal of Materials Science*, vol. 18, no. 7, pp. 1423–1432, 2007.
- [5] J. Ge, J. Qian, X. Wang et al., "Effectiveness and safety of the sirolimus-eluting stents coated with bioabsorbable polymer coating in human coronary arteries," *Catheterization and Cardiovascular Interventions*, vol. 69, no. 2, pp. 198–202, 2007.
- [6] K. J. Winters, S. C. Smith, M. Cohen, C. Kopistansky, and R. McBride, "Reduction in ischemic vascular complications with a hydrophilic-coated intra-aortic balloon catheter," *Catheterization and Cardiovascular Interventions*, vol. 46, no. 3, pp. 357–362, 1999.
- [7] B. Scheller, U. Speck, C. Abramjuk, U. Bernhardt, M. Böhm, and G. Nickenig, "Paclitaxel balloon coating, a novel method for prevention and therapy of restenosis," *Circulation*, vol. 110, no. 7, pp. 810–814, 2004.
- [8] B. Scheller, C. Hehrlein, W. Bocksch et al., "Treatment of coronary in-stent restenosis with a paclitaxel-coated balloon catheter," *The New England Journal of Medicine*, vol. 355, no. 20, pp. 2113–2124, 2006.
- [9] B. Scheller, U. Speck, B. Romeike et al., "Contrast media as carriers for local drug delivery: successful inhibition of

- neointimal proliferation in the porcine coronary stent model," *European Heart Journal*, vol. 24, no. 15, pp. 1462–1467, 2003.
- [10] B. Cremers, Y. Clever, S. Schaffner, U. Speck, M. Böhm, and B. Scheller, "Treatment of coronary in-stent restenosis with a novel paclitaxel urea coated balloon," *Minerva Cardioangiologica*, vol. 58, no. 5, pp. 583–588, 2010.
- [11] B. Kelsch, B. Scheller, M. Biedermann et al., "Dose response to Paclitaxel-coated balloon catheters in the porcine coronary overstretch and stent implantation model," *Investigative Radiology*, vol. 46, no. 4, pp. 255–263, 2011.
- [12] M. C. Berg, H. Kolodziej, B. Cremers, G. Gershony, and U. Speck, "Drug-coated angioplasty balloon catheters: coating compositions and methods," *Advanced Engineering Materials*, vol. 14, no. 3, pp. B45–B50, 2012.
- [13] E. A. Balazs, "Hyaluronan as an ophthalmic viscoelastic device," *Current Pharmaceutical Biotechnology*, vol. 9, no. 4, pp. 236–238, 2008.
- [14] E. J. Strauss, J. A. Hart, M. D. Miller, R. D. Altman, and J. E. Rosen, "Hyaluronic acid viscosupplementation and osteoarthritis: current uses and future directions," *The American Journal of Sports Medicine*, vol. 37, no. 8, pp. 1636–1644, 2009.
- [15] D. R. Friedland and C. Runge-Samuels, "Soft cochlear implantation: rationale for the surgical approach," *Trends in Amplification*, vol. 13, no. 2, pp. 124–133, 2009.
- [16] J. A. Yang, E. S. Kim, J. H. Kwon et al., "Transdermal delivery of hyaluronic acid—human growth hormone conjugate," *Biomaterials*, vol. 33, no. 25, pp. 5947–5954, 2012.
- [17] T. Nakai, T. Hirakura, Y. Sakurai, T. Shimoboji, M. Ishigai, and K. Akiyoshi, "Injectable hydrogel for sustained protein release by salt-induced association of hyaluronic acid nanogel," *Macromolecular Bioscience*, vol. 12, no. 4, pp. 475–483, 2012.
- [18] H. Schlicht and E. Wintermantel, "Single-Use Instrumente in der endoskopischen Gastroenterologie," in *Medizintechnik: Life Science Engineering*, E. Wintermantel and S. W. Ha, Eds., pp. 1189–1214, Springer, Berlin, Germany, 2009.
- [19] A. Baumbach, C. Herdeg, M. Kluge et al., "Local drug delivery: impact of pressure, substance characteristics, and stenting on drug transfer into the arterial wall," *Catheterization and Cardiovascular Interventions*, vol. 47, no. 1, pp. 102–106, 1999.
- [20] M. N. Collins and C. Birkinshaw, "Investigation of the swelling behavior of crosslinked hyaluronic acid films and hydrogels produced using homogeneous reactions," *Journal of Applied Polymer Science*, vol. 109, no. 2, pp. 923–931, 2008.
- [21] A. Ulman, "Formation and structure of self-assembled monolayers," *Chemical Reviews*, vol. 96, no. 4, pp. 1533–1554, 1996.
- [22] I. Luzinov, D. Julthongpipit, A. Liebmann-Vinson, T. Cregger, M. D. Foster, and V. V. Tsukruk, "Epoxy-terminated self-assembled monolayers: molecular glues for polymer layers," *Langmuir*, vol. 16, no. 2, pp. 504–516, 2000.
- [23] W. G. Pitt, R. N. Morris, M. L. Mason, M. W. Hall, Y. Luo, and G. D. Prestwich, "Attachment of hyaluronan to metallic surfaces," *Journal of Biomedical Materials Research A*, vol. 68, no. 1, pp. 95–106, 2004.
- [24] M. N. Collins and C. Birkinshaw, "Comparison of the effectiveness of four different crosslinking agents with hyaluronic acid hydrogel films for tissue-culture applications," *Journal of Applied Polymer Science*, vol. 104, no. 5, pp. 3183–3191, 2007.
- [25] K. Tomihata and Y. Ikada, "Preparation of cross-linked hyaluronic acid films of low water content," *Biomaterials*, vol. 18, no. 3, pp. 189–195, 1997.
- [26] X. B. Zhao, J. E. Fraser, C. Alexander, C. Lockett, and B. J. White, "Synthesis and characterization of a novel double crosslinked hyaluronan hydrogel," *Journal of Materials Science*, vol. 13, no. 1, pp. 11–16, 2002.
- [27] L. Cen, K. G. Neoh, and E. T. Kang, "Surface functionalization of electrically conductive polypyrrole film with hyaluronic acid," *Langmuir*, vol. 18, no. 22, pp. 8633–8640, 2002.
- [28] S. Mädler, C. Bich, D. Touboul, and R. Zenobi, "Chemical cross-linking with NHS esters: a systematic study on amino acid reactivities," *Journal of Mass Spectrometry*, vol. 44, no. 5, pp. 694–706, 2009.
- [29] A. Bohl, H. W. Rohm, P. Ceschi et al., "Development of a specially tailored local drug delivery system for the prevention of fibrosis after insertion of cochlear implants into the inner ear," *Journal of Materials Science*, vol. 23, no. 9, pp. 2151–2162, 2012.
- [30] J. K. Jackson, K. C. Skinner, L. Burgess, T. Sun, W. L. Hunter, and H. M. Burt, "Paclitaxel-loaded crosslinked hyaluronic acid films for the prevention of postsurgical adhesions," *Pharmaceutical Research*, vol. 19, no. 4, pp. 411–417, 2002.
- [31] J. M. Goddard and J. H. Hotchkiss, "Polymer surface modification for the attachment of bioactive compounds," *Progress in Polymer Science*, vol. 32, no. 7, pp. 698–725, 2007.



Hindawi

Submit your manuscripts at
<http://www.hindawi.com>

